AIAA JOURNAL
Vol. 33, No. 10, October 1995

Low-Speed Impact Damage-Initiation Characteristics of Selected Laminated Composite Plates

Damodar R. Ambur* and James H. Starnes Jr.†
NASA Langley Research Center, Hampton, Virginia 23681-0001
and
Chunchu B. Prasad‡
Analytical Services and Materials, Inc., Hampton, Virginia 23666

The results of an experimental and analytical study of damage initiation in laminated composite plates subjected to low-speed impact are presented. Here, 8-, 16-, 24-, 32-, and 48-ply-thick quasi-isotropic and orthotropic graphite-epoxy and graphite-bismaleimide laminated plates have been impacted with dropped weights and the corresponding plate responses have been predicted analytically. Impact damage-initiation thresholds and damage-initiation mechanisms corresponding to a range of impact-energy levels are identified. Impact-damage initiation for the thicker plates occurs at both the impact site and the plate surface opposite to the impact site. Impact-damage initiation for the thinner plates is predominately due to tensile fracture on the plate surface opposite to the impact site. Three-dimensional stress states that correspond to the impact conditions that initiate damage are determined analytically to help identify damage-initiation mechanisms and to predict failure-initiation modes.

Introduction

THE effect of low-speed impact damage on the compression strength of laminated composite structures has been studied extensively by many researchers over the past several years and the results of these studies are summarized in Ref. 1. Test data show that the compression strength of composite structures can be significantly reduced by low-speed impact damage, even if the damage is not detectable by visual inspection. The sensitivity of the compression strength of composite structures to low-speed impact damage has led to the development of more damage-resistant material systems, of damage-tolerant material architectures such as materials with through-the-thickness reinforcement, and of special damage-tolerance design criteria for composite airframe structures. To determine the damage resistance of laminated composite structures, which can be represented by the impact-energy level that initiates damage, it is necessary to understand both the impact parameters and the plate parameters that influence plate response. Insight into the transient dynamic response of impacted composite plates is necessary to distinguish between different failure mechanisms and to improve the performance of composite structures. Such insight will also contribute to the development of test methods that can be used to help select materials with better impact-damage resistance for structural applications.

Several researchers have studied low-speed impact-damage failure modes and the resistance of laminated composite plates to low-speed impact damage (e.g., Refs. 2–12). Most of this earlier work was experimental, and both nondestructive and destructive inspection methods were used to investigate differences in failure modes. Predicting failure initiation analytically by estimating the three-dimensional transient stress state in an impacted composite plate has been addressed by only a few researchers. Failure criteria were used in these studies to predict the damage-initiation modes and locations in an impacted composite plate. Some of these analytical studies were part of analytical methods development efforts and the accuracy of the methods was not established. Understanding the influence of both impact and plate parameters on impact-damage resistance is still evolving, and analytical methods that reliably predict damage initiation are still being developed.

The present paper presents the results of an experimental and analytical study of damage initiation in laminated composite plates subjected to low-speed impact. Here, 8-, 16-, 24-, 32-, and 48-ply-thick quasi-isotropic and orthotropic graphite-epoxy and graphite-bismaleimide laminated plates have been impacted with dropped weights to determine impact-damage initiation thresholds, damage resistance, and damage mechanisms that correspond to a range of impact-energy levels. The closed-form transient plate analysis developed in Ref. 13 is used to predict plate impact response and the three-dimensional stress states corresponding to damage-initiation impact-energy levels. Analytical results are compared with experimental results to evaluate the accuracy of the analysis method. Observed failure-initiation modes for typical composite plates are compared with analytical results, and limitations of the analysis procedure to predict transient plate response are discussed.

Analysis Method

A brief description of the transient analysis used to determine the in-plane and interlaminar stresses in laminated composite plates subjected to low-speed impact and the failure criteria used to predict damage-initiation modes are described in this section.

In-Plane Stresses

The in-plane stresses in an impacted composite plate are determined from the transient analysis of the plate response presented in Ref. 13. The transient deformations of the plate [Eqs. (18) in Ref. 13] and the corresponding strain-displacement relations are used to determine the plate midplane strains. The stains in the midplane of each ply are then determined by assuming that the ply midplane is located at a distance z from the plate midplane and the in-plane stresses σ_x, σ_y, and τ_{xy} in each ply are determined from the strains in the ply using the constitutive relations for the composite material. These stresses are then transformed into the ply principal stresses σ_{11}, σ_{22}, and σ_{12} in the ply fiber direction.

Interlaminar Stresses

The interlaminar stresses σ_z, σ_{xy}, and σ_{yz} in the plate are determined from the governing equilibrium equations for the plate given

Received March 2, 1994; revision received Feb. 6, 1995; accepted for publication Feb. 20, 1995.

*Senior Aerospace Engineer, Structural Mechanics Branch. Associate Fellow AIAA.
†Head, Structural Mechanics Branch. Fellow AIAA.
‡Research Engineer. Member AIAA.

in Ref. 14 with the appropriate stress boundary conditions. The resulting interlaminar stresses are given by

$$\sigma_z = (h^3/48)\{[1+(2z/h)^3]-3[1+(2z/h)]\} \times \{[\alpha^3 Q_{11}+\alpha\beta^2(2G_{12}+Q_{12})]X + [(2G_{12}+Q_{12})\alpha^2\beta+\beta^3 Q_{22}]Y\}\sin\alpha x\sin\beta y$$

$$\sigma_{xz} = -(h^2/8)[1-(2z/h)^2] \times \{[\alpha^2 Q_{11}+\beta^2 G_{12}]X+[G_{12}+Q_{12}]\alpha\beta Y\}\cos\alpha x\sin\beta y$$

$$\sigma_{yz} = -(h^2/8)[1-(2z/h)^2] \times \{[\alpha^2 G_{12}+\beta^2 Q_{22}]Y+[G_{12}+Q_{12}]\alpha\beta X\}\sin\alpha x\cos\beta y$$

where $\alpha = m\pi/a, \beta = n\pi/b, X = X_{mn}$, and $Y = Y_{mn}$. The coefficients X_{mn} and Y_{mn} are given by Eq. (8) in Ref. 13. The terms Q_{ij} are the elastic constants based on a plane-stress assumption for specially orthotropic plates and are derived from the elastic moduli of the laminated plate in body coordinates. The transverse shear stresses σ_{xz} and σ_{yz} are transformed into the interlaminar shear stresses σ_{13} and σ_{23} in the ply fiber direction. This three-dimensional stress state is used to evaluate the initial failure modes for the impacted plates in the present study.

Failure Criteria

Two different failure criteria have been used for predicting failure initiation in the impacted laminated plates. These criteria are the maximum stress criterion and the quadratic failure criterion suggested by Hashin.[15] The maximum stress failure criterion addresses failure due to individual stress components in each ply. The quadratic failure criterion is a three-dimensional failure criterion that takes into account the interaction of all six stress components. The quadratic failure criterion is more conservative than the maximum stress criterion for determining critical failure modes.

Test Specimens and Experimental Method

The specimens tested in the present study were fabricated from 0.005-in.-thick AS4/3502 graphite-epoxy or 0.005-in.-thick IM7/5260 graphite-bismaleimide preimpregnated unidirectional tape materials. The AS4 and IM7 graphite fibers and the 3502 epoxy resin are made by Hercules, Inc., and the 5260 bismaleimide resin is made by BASF, Inc. All specimens were cured in an autoclave using the resin manufacturers' recommended procedures. The AS4/3502 specimens were made with either $[45/0/-45/90]_{ns}$ quasi-isotropic, $[\pm 45_2/90_2/\pm 45_2/0_2/\pm 45/0/\pm 45_2/90/\pm 45_2]_s$ orthotropic (designated as the type C laminate herein), or $[\pm 45_2/90_2/\pm 45_2/0_3/\pm 45/0_2/\pm 45_2/90/\pm 45]_s$ orthotropic (designated as the type D laminate herein) stacking sequences. The quasi-isotropic specimens were 8-, 16-, 24-, 32-, and 48-plies thick. The orthotropic laminates (types C and D) are commonly used lamination sequences in current aircraft structures. The IM7/5260 specimens were made with 24-, 32- or 48-ply-thick quasi-isotropic stacking sequences. Typical mechanical properties for these material systems are listed in Table 1. All specimens were 5 in. wide and 10 in. long. Identification of commercial products and companies in the present paper is used to describe the test specimens adequately. The identification of these commercial products does not constitute endorsement, expressed or implied, of such products by NASA.

The specimens were simply supported on all four edges and impacted by dropping a weight onto the specimen from a prescribed height. Specimens of each laminate were impacted with increasing impact-energy levels until damage initiation was detected. The 8-, 16- and 24-ply-thick specimens were impacted in 0.25 ft-lb increments of increasing impact energy, and the 32- and 48-ply-thick specimens were impacted in 0.5 ft-lb increments of increasing impact energy. The specimens were visually inspected and ultrasonically C scanned after each impact event to determine if damage initiation had occurred, and this process was repeated until the impact-energy level necessary to initiate damage in the specimen was identified. A volumetric ultrasonic imaging technique[9] was used to identify the damage-initiation modes of the specimens nondestructively. Some specimens were cross sectioned, and photomicrography was used to identify the damage in these specimens. Once the damage-initiation impact-energy level was determined for a given specimen, an identical undamaged specimen was instrumented, as shown in Fig. 1, and impacted in the center of the plate to obtain the contact force and in-plane strain data. This specimen was also used for a final characterization of the impact damage. Surface strains, contact forces, and displacements were measured with strain gauges and force and displacement transducers for all tests, and the data were recorded electronically. A high-speed storing oscilloscope was used to record the transient response data as a function of time.

Table 1 Typical mechanical properties of unidirectional tape materials

Property	Material AS4/3502	IM7/5260	T300/934
Longitudinal modulus, E_1, Msi	20.00	22.20	21.09
Transverse modulus, E_2, Msi	1.30	1.30	1.45
In-plane shear modulus, G_{12}, Msi	0.87	0.74	0.82
Transverse shear modulus, G_{23}, Msi	0.50	0.48	0.82
Transverse shear modulus, G_{13}, Msi	0.87	0.55	0.82
Major Poisson's ratio, ν_{12}	0.30	0.29	0.30
Nominal ply thickness, in.	0.005	0.005	0.006
Longitudinal tensile strength, S_{lt}, ksi	322.00		
Longitudinal compressive strength, S_{lc}, ksi	230.00		
Transverse tensile strength, S_{tt}, ksi	8.40		
Transverse compressive strength, S_{tc}, ksi	16.40		
Transverse shear strength, S_{ts}, ksi	17.00		
Interlaminar shear strength, S_{ss}, ksi	11.60		

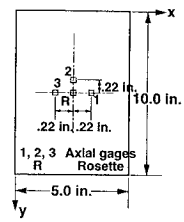

Fig. 1 Strain gauge instrumentation details for the impact specimens.

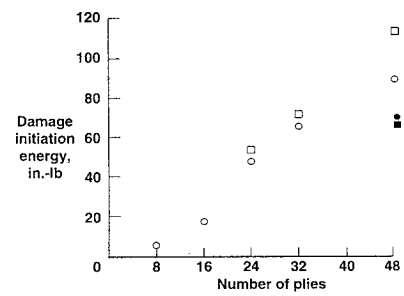

Fig. 2 Summary of dropped weight impact-damage-initiation levels: ○, AS4/3502 graphite-epoxy, QI laminate ($[45/0/-45/90]_{ns}$); □, IM7/5260 graphite-bismaleimide, QI laminate ($[45/0/-45/90]_{ns}$); ●, AS4/3502 graphite-epoxy, Type C laminate 75 percent ±45 deg plies; ■, AS4/3502 graphite-epoxy, Type D laminate 66 percent ±45 deg plies.

Results and Discussion

Damage-initiation impact-energy levels obtained as an average from three tests for each of the AS4/3502 and IM7/5260 quasi-isotropic specimens are presented in Fig. 2 as a function of specimen

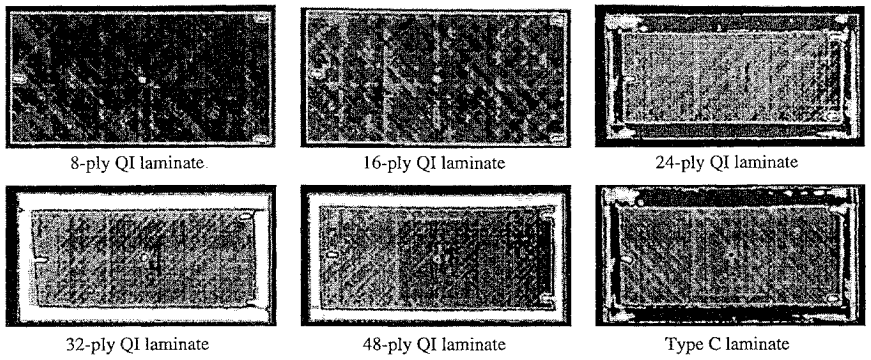

Fig. 3 Ultrasonic C-scan results of specimens showing damaged sites.

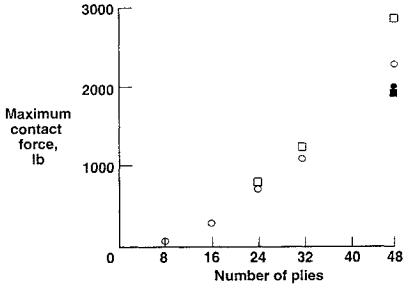

Fig. 4 Maximum contact-force values for damage initiation in quasi-isotropic plates: ○, AS4/3502 graphite-epoxy, QI laminate ($[45/0/-45/90]_{ns}$); □, IM7/5260 graphite-bismaleimide, QI laminate ($[45/0/-45/90]_{ns}$); ●, AS4/3502 graphite-epoxy, Type C laminate 75 percent ±45 deg plies; ■, AS4/3502 graphite-epoxy, Type D laminate 66 percent ±45 deg plies.

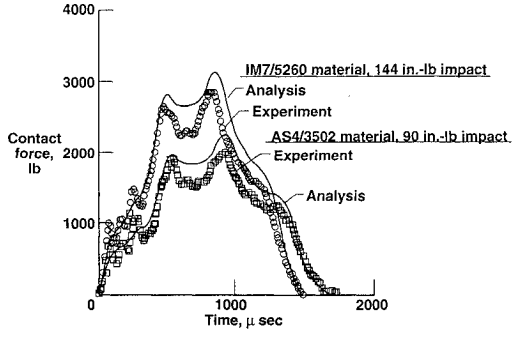

a) Contact force profiles

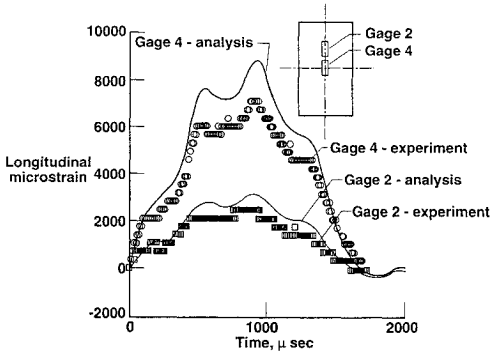

b) Axial strain profiles

Fig. 5 Dropped weight impact response of 48-ply-thick graphite-epoxy quasi-isotropic plates at impact-damage-initiation threshold energy level.

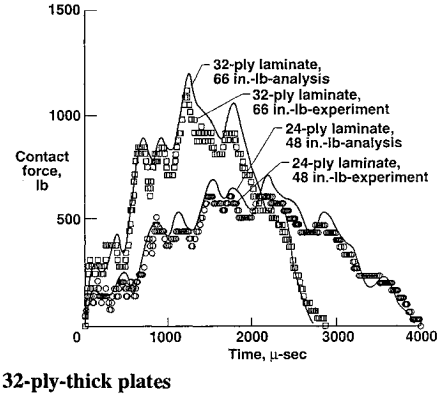

a) 24- and 32-ply-thick plates

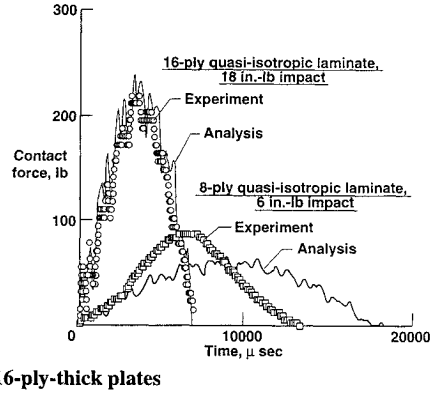

b) 8- and 16-ply-thick plates

Fig. 6 Contact force profiles for graphite-epoxy quasi-isotropic plates subjected to dropped weight impact at impact-damage-initiation threshold energy levels.

thickness (number of plies in the laminate). The impact-energy level required for damage initiation increases as a function of laminate thickness for specimens made of both material systems. This trend is similar to the one reported in Refs. 1 and 8. The specimens made from the tougher IM7/5260 material system exhibit better damage resistance than the specimens made from the AS4/3502 material system. The difference in the slopes of the trends of the data for these two material systems indicate that the common practice of using impact energy per unit laminate thickness as a basis for comparing the damage tolerance characteristics of composite structures made of different material systems is questionable. The trends in these data appear to be not only nonlinear, but they are different in nature for the two material systems over the range of specimen thicknesses considered herein. The damage-initiation impact-energy levels for specimens with the type C (75% ±45-deg plies) and type D (66% ±45-deg plies) laminates are lower than the damage-initiation impact-energy levels for the 48-ply-thick quasi-isotropic specimens. The types C and D specimens have a much higher percentage of ±45-deg plies than the quasi-isotropic specimens and are generally considered to have a higher damage-initiation threshold level

than the quasi-isotropic specimens. The stacking sequences used for the orthotropic specimens apparently make these specimens more susceptible to low-speed impact damage than the quasi-isotropic specimens with the same thickness. Ultrasonic C-scan results that illustrate the extent of damage corresponding to the impact-damage-initiation threshold energy levels for the different specimens are presented in Fig. 3.

The maximum values of the measured contact force corresponding to damage initiation in the AS4/3502 and IM7/5260 quasi-isotropic plates of different thicknesses are shown in Fig. 4. The trends for these data suggest that the contact force is a nonlinear function of the plate thickness and that a simple linear relationship between the plate thickness and the contact force is not representative of plate behavior for laminated plates made of different material systems. The measured and analytically predicted contact force and longitudinal strain results for the 48-ply-thick AS4/3502 and IM7/5260 quasi-isotropic plates are presented in Fig. 5, and the results correlate well. These results correspond to the impact-energy levels at which damage initiates in the plates and noticeable matrix compression failure occurs at the impact site due to high transverse normal stresses caused by the contact force. Even though this local damage can cause a change in contact stiffness, the contact force results presented in Fig. 5a correlate well. The surface strains predicted at strain gauge locations 2 and 4 also compare well with the measured strains as shown in Fig. 5b.

Experimental and analytical contact force results are presented in Fig. 6 for the 8-, 16-, 24-, and 32-ply-thick AS4/3502 plates. Some matrix compression failure was observed at the impact site for the 32-ply-thick specimen. The predominate failure mode for the 8-, 16-, and 24-ply-thick specimens is a local tensile matrix failure on the specimen surface opposite to the impact site. The experimental and analytical contact force results for the 16-, 24-, and 32-ply-thick plates correlate well. The experimental and analytical contact force results presented in Fig. 6b for the 8-ply-thick plate do not correlate very well. Experimental and analytical surface strain results are presented in Fig. 7 for the 24- and 32-ply-thick plates.

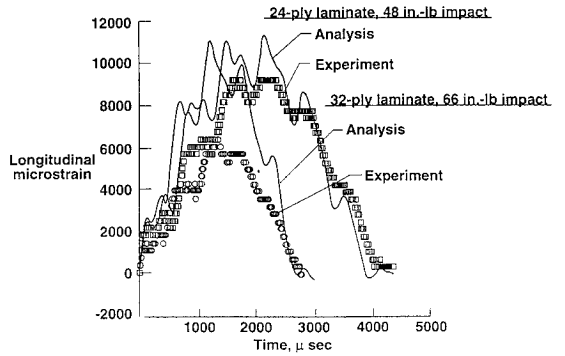

Fig. 7 Comparison of axial strains for 24- and 32-ply-thick quasi-isotropic laminates subjected to dropped weight impact at impact-damage-initiation threshold energy levels.

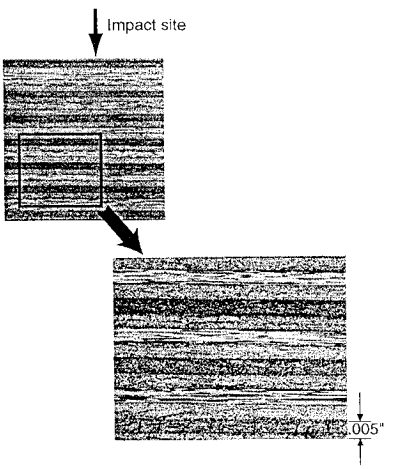

a) 48-ply-thick plate

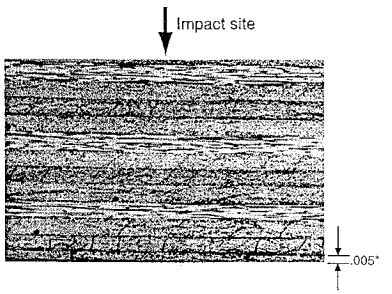

b) 32-ply plate (13 plies shown from the bottom of the plate)

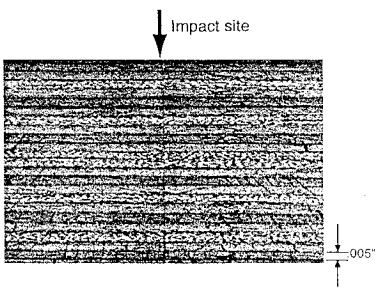

c) 24-ply-thick plate

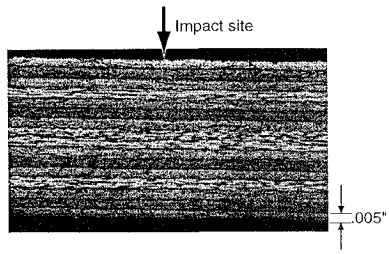

d) 16-ply-thick plate

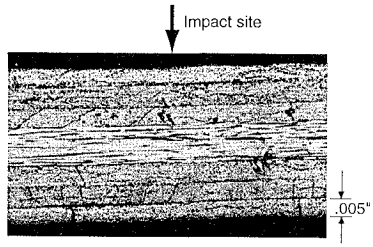

e) 8-ply-thick plate

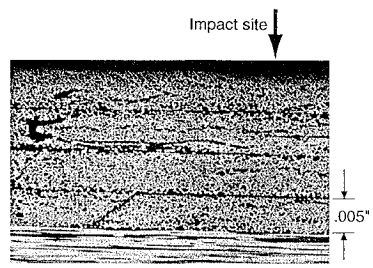

f) Type C plate (6 plies shown from the bottom of the plate)

Fig. 8 Photomicrographs of quasi-isotropic plate subjected to dropped-weight impact damage.

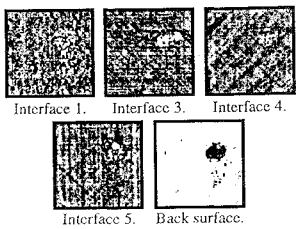

a) Quasi-isotropic plate

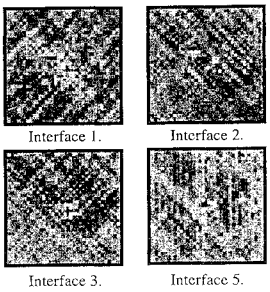

b) Type C plate

Fig. 9 Through-the-thickness ultrasonic images for 48-ply laminates.

These results indicate that nonlinear effects influence the response of specimens that are equal to or thinner than 24 plies even at the low-impact-energy levels that correspond to damage initiation. The analysis used in the present paper to predict failure initiation is based on small-deflection theory and, as a result, has only been used to predict failure initiation for the 32- and 48-ply-thick plates.

Photomicrographs of specimen cross sections through the impact site are presented in Fig. 8 for AS4/3502 quasi-isotropic specimens of different thicknesses. A considerable region of matrix compression failure is observed at the impact site for the 32- and 48-ply-thick specimens that may lead to subsequent delaminations and reductions in bending stiffnesses. Extensive matrix tensile failure is apparent in the plies that are close to the surface of the laminate opposite to the impact site for these specimens. The damage in the 8- and 16-ply-thick specimens is predominately in the plies near the surface opposite to the impact site. Matrix tensile failures that may result in delaminations at the ply interfaces are apparent for these specimens. This failure mode is to be expected in thin laminates since they are subjected to a considerable amount of local bending due to impact. The damage to the orthotropic type C specimen is matrix compression failure in the plies near the impact site and some local delaminations. The largest observed delamination is located between the third and fourth plies in from the impacted surface. Typical ultrasonic C-scan images for 48-ply-thick AS4/3502 quasi-isotropic and orthotropic type C specimens are shown in Fig. 9. The numbers indicated at the bottom of each figure correspond to ply interfaces represented in the figure. For example, interface number 1 refers to the interface between the first 45-deg and 0-deg plies for the quasi-isotropic specimen. As shown in the figure, damage only extends into the fifth ply interface for this 48-ply-thick specimen. The dominant failure mode for this specimen appears to be delamination at all of the affected interfaces. The largest observed damage for the orthotropic type C specimen occurs at the third ply interface that is consistent with the results shown in the photomicrograph. These results suggest that enough local damage occurs in these specimens at the damage-initiation threshold impact-energy levels to reduce the local stiffnesses of the plates and, as a result, to affect the subsequent transient response of the plate and corresponding damage propagation.

Validation of Analytical Three-Dimensional Stress Predictions

The analytical method used in the present study to predict interlaminar stresses and failure initiation in plates subjected to low-speed impact is based on a plane-stress assumption and, as a result, is not expected to predict the through-the-thickness normal stresses accurately. However, the interlaminar shear stress predictions are expected to be reasonable approximations of the stresses in the plate. To determine the quality of the present two-dimensional analysis

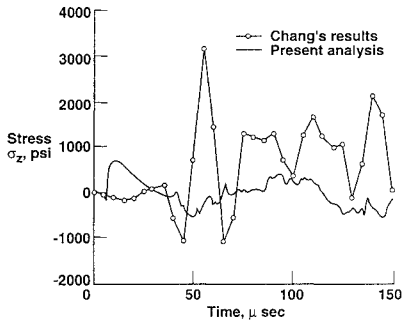

Fig. 10 Comparison of panel impact response results between the present analysis and a finite element analysis.

results, the magnitudes and distribution of the interlaminar stresses from the present analysis are compared in Figs. 10 and 11 with results from a three-dimensional finite element analysis provided by F. K. Chang from Stanford University. These results are for a simply supported 3.0-in.-square T300/934 graphite-epoxy plate with a $[0/-45/45/90]_{2s}$ stacking sequence that is impacted by a 0.5-in.-diam aluminum ball with a speed of 1000 in./s from an air gun. Nominal mechanical properties used in the analysis for the T300/934 graphite-epoxy material system are presented in Table 1. The interlaminar normal stress profile corresponding to this low-speed impact at the midpoint (i.e., $x = 1.5$ in. and $y = 1.5$ in.) of the plate is shown in Fig. 10. The magnitude and phase of the interlaminar normal stress from the present analysis is much lower than the finite element analysis result. The through-the-thickness in-plane and interlaminar stress results near the impact site (i.e., $x = 1.2$ in. and $y = 1.8$ in.) at 25 μs are shown in Fig. 11. The trends for all of the stress components compare well except for the interlaminar normal stresses. The differences in the results shown in Fig. 11 are due to the differences in the normal stress profiles obtained from the two analyses shown in Fig. 10. This normal stress profile is for the second ply in from the impacted surface. Some of the differences in the results may also be due to differences in the models used for the two analyses. Model fidelity and refinement are particularly critical for transient impact problems since steep stress gradients exist in the vicinity of the impact location. The number of terms used in the present analysis to determine the interlaminar stresses is based on the number of terms necessary to obtain convergence for the in-plane stresses.

Prediction of Failure Initiation Modes

Since results from the present two-dimensional analysis are reasonably consistent with results from a three-dimensional finite element analysis, the present analysis was used to estimate the three-dimensional stress state for a 48-ply-thick AS4/3502 quasi-isotropic plate at the damage-initiation threshold impact-energy level. The strength data presented in Table 1 for this material system were used in conjunction with the maximum-stress and quadratic failure criteria to identify failure-initiation modes for this impact condition. To conduct the analyses, a model was generated with a network of grid points distributed through-the-thickness of the plate and along radial lines in the plane of the plate that extend outward from the impact site. The failure criteria were applied at each of these grid points as the transient impact response developed with time, and the initiation of failure was identified at the critical point. Results from this limited study of a plate impacted at its center suggest that matrix compression failure occurs at points up to a radius of 0.1 in. away from the impact site. This region of compression failure is greater than the impactor contact radius of 0.055 in. The damage region for matrix tension failure is comparable to the matrix compression failure region. Matrix compression failure is predicted to occur in the eight plies in from the impacted surface and matrix tensile failure is predicted to occur in the eight plies in from the surface opposite to the impact site. These results indicate that the maximum-stress failure criterion predicts matrix failure to occur much later into the impact event (where the contact forces are larger) than the quadratic failure criterion. The photomicrographs and ultrasonic C scans indicate that matrix failure and related delaminations occur up to five

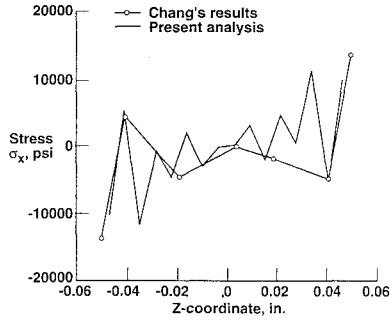

a) Longitudinal stress distribution

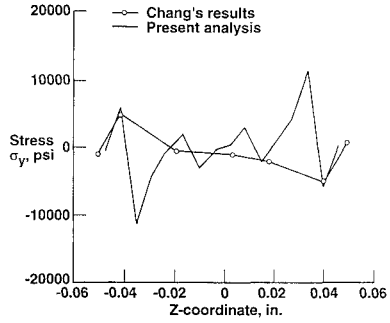

b) Transverse axial stress distribution

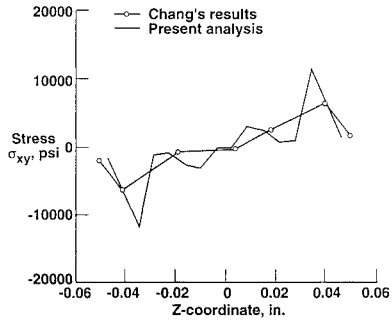

c) In-plane shear stress distribution

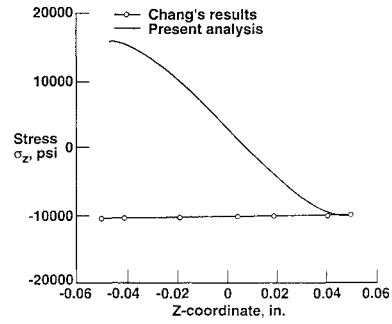

d) Transverse normal stress distribution

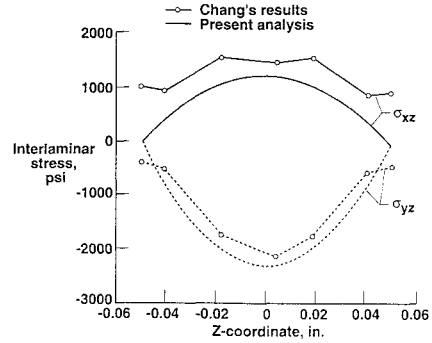

e) Transverse shear stress distribution in the laminate xz and yz planes

Fig. 11 Comparison of three-dimensional stress results through the thickness of a 0.1-in.-thick 16-ply quasi-isotropic plate for the present analysis and a finite element analysis.

plies in from the impacted surface and up to three plies in from the surface opposite to the impact site. The smaller extent of damage observed in the tests may be related to the amount of energy absorbed by the plate when the matrix cracks, and delaminations are created during the damage-initiation process that are not accounted for in the present analysis.

Concluding Remarks

Experimental studies have been conducted to determine the threshold impact-energy levels necessary to initiate damage in laminated composite plates made of different materials and lamination sequences and subjected to low-speed impact. The impact energy for damage initiation is a nonlinear function of the plate thickness and has a different nonlinear relationship for laminated plates made of different material systems. These results suggest that a linear relationship based on impact energy per unit thickness may not be appropriate for comparing results for different laminate thicknesses or material systems. The contact force corresponding to these damage-initiation impact-energy levels is also a nonlinear function of plate thickness that indicates that using contact force as a parameter for determining relative damage-initiation levels or damage resistance should be based on a set of well-defined laminate parameters.

The failure-initiation modes corresponding to the impact-energy threshold level for damage initiation are predominately matrix related failures which may lead to the delamination failures typically observed in low-speed impact tests. Impact-damage initiation for the 32- and 48-ply-thick plates tested in the present study occurred both at the impact site and on the surface opposite to the impact site. Impact-damage initiation in the 24-ply-thick and thinner plates occurred mostly on the surface opposite to the impact site. Two-dimensional small-deflection transient plate analysis results were compared with three-dimensional analysis results and used to correlate with the experimental results of the study. These results were also used to determine failure initiation based on two failure criteria. The two-dimensional analysis results compared well with the three-dimensional analysis results except for the interlaminar normal stresses. Experimental and analytical results for the thicker plates correlated well, but results for the thinner plates indicate that nonlinear effects can be significant for the thinner plates and should be included in the analysis. The two-dimensional analysis predicted the observed impact-damage initiation modes for the thicker 48-ply-thick plates which were predominantly matrix compression failure on the impacted surface and matrix tension failure on the surface opposite to the impact site. The extent of local damage near the impact site is also well predicted by the present analysis. These results suggest that failure initiation may be predictable analytically. Subsequent failure propagation due to low-speed impact may be predictable analytically in the future if critical failure modes and local damage propagation effects are properly included in the analysis.

Acknowledgment

The authors thank F. K. Chang, School of Aeronautics and Astronautics, Stanford University, for making available his three-dimensional analysis results that were used by the authors to verify their two-dimensional analysis results.

References

[1]Abrate, S., "Impact on Laminated Composite Materials," *Applied Mechanics Reviews*, Vol. 44, No. 4, 1991, pp. 155–190.

[2]Starnes, J. H., Jr., Rhodes, M. D., and Williams, J. G., "Effect of Impact Damage and Holes on the Compressive Strength of a Graphite/Epoxy Laminate," *Nondestructive Evaluation and Flaw Criticality for Composite Materials*, edited by R. B. Pipes, American Society for Testing and Materials, ASTM STP 696, 1979, pp. 145–171.

[3]Joshi, S. P., and Sun, C. T., "Impact Induced Fracture in a Laminated Composite," *Journal of Composite Materials*, Vol. 19, Jan. 1985, pp. 51–66.

[4]Guynn, E. G., and O'Brien, T. K., "The Influence of Lay-Up and Thickness on Composite Impact Damage and Compression Strength," *Proceedings of the AIAA/ASME/ASCE/AHS 26th Structures, Structural Dynamics and Materials Conference* (Orlando, FL), AIAA, New York, 1985, pp. 187–196.

[5]Elber, W., "The Effect of Matrix and Fiber Properties on Impact Resistance," *Tough Composite Materials: Recent Developments*, Noyes, Park Ridge, NJ, 1985, pp. 89–110.

[6]Gause, L. W., and Buckley, L. J., "Impact Characterization of New Composite Materials," *Instrumented Impact Testing of Plastics and Composite Materials*, American Society for Testing and Materials, ASTM STP 939, 1987, pp. 248–261.

[7]Wu, H. T., and Springer, G. S., "Measurements of Matrix Cracking and Delamination Caused by Impact on Composite Plates," *Journal of Composite Materials*, Vol. 22, June 1988, pp. 518–532.

[8]Cantwell, W. J., and Morton, J., "Geometrical Effectsin the Low Velocity Impact Response of CFRP," *Composite Structures*, Vol. 12, No. 1, 1989, pp. 39–59.

[9]Smith, B. T., et al., "Correlation of the Deply Technique with Ultrasonic Imaging of Impact Damage in Graphite-Epoxy Composites," *Materials Evaluation, Journal of the American Society for Nondestructive Testing*, Vol. 47, No. 12, 1989, pp. 1408–1416.

[10]Wang, C.-Y., and Yew, C.-H., "Impact Damage Composite Laminates," *Computers and Structures*, Vol. 37, No. 6, 1990, pp. 967–982.

[11]Lin, H. J., and Lee, Y. J., "Impact-induced Fracture in Laminated Plates and Shells," *Journal of Composite Materials*, Vol. 24, Nov. 1990, pp. 1179–1199.

[12]Lee, S. M., and Zahuta, P., "Instrumented Impact and Static Indentation of Composites," *Journal of Composite Materials*, Vol. 25, Feb. 1991, pp. 204–222.

[13]Ambur, D. R., Starnes, J. H., Jr., and Prasad, C. B., "Influence of Transverse Shear and Large Deformation Effects on the Low-Speed Impact Response of Laminated Composite Plates," NASA TM-107753, April 1993.

[14]Reddy, J. N., "A Refined Nonlinear Theory of Plates with Transverse Shear Deformation," *International Journal of Solids and Structures*, Vol. 20, No. 9–10, 1984, pp. 881–896.

[15]Hashin, Z., "Failure Criteria for Unidirectional Fiber Composites," *Journal of Applied Mechanics*, Vol. 47, June 1980, pp. 329–334.